OXFORD

PART I

Fluid Dynamics

CLASSICAL FLUID DYNAMICS

Anatoly I. Ruban
AND Jitesh S. B. Gajjar

Fluid Dynamics

Part 1: Classical Fluid Dynamics

Anatoly I. Ruban
Department of Mathematics
Imperial College London

Jitesh S. B. Gajjar
School of Mathematics
University of Manchester

OXFORD
UNIVERSITY PRESS

OXFORD
UNIVERSITY PRESS

Great Clarendon Street, Oxford, OX2 6DP,
United Kingdom

Oxford University Press is a department of the University of Oxford.
It furthers the University's objective of excellence in research, scholarship,
and education by publishing worldwide. Oxford is a registered trade mark of
Oxford University Press in the UK and in certain other countries

First Edition published in 2014

Impression: 1

Published in the United States of America by Oxford University Press
198 Madison Avenue, New York, NY 10016, United States of America

British Library Cataloguing in Publication Data
Data available

Library of Congress Control Number: 2013953774

ISBN 978–0–19–968173–0

Printed in Great Britain by
Clays Ltd, St Ives plc

Fluid Dynamics

Preface

This book is the first of a series on fluid dynamics that will comprise the following four parts:

Part 1. Classical Fluid Dynamics

Part 2. Asymptotic Problems of Fluid Dynamics

Part 3. Boundary Layers

Part 4. Hydrodynamic Stability Theory

The series is designed to give a comprehensive and coherent description of fluid dynamics, starting with chapters on classical theory suitable for an introductory undergraduate lecture course, and then progressing through more advanced material up to the level of modern research in the field. Our main attention will be on high-Reynolds-number flows, both incompressible and compressible. Correspondingly, the target reader groups are undergraduate and MSc students reading mathematics, aeronautical engineering, or physics, as well as PhD students and established researchers working in the field.

Over the last 50 years, there have been major advances in various aspects of fluid dynamics. In particular, significant progress has been achieved in understanding the behaviour of compressible fluid flows, including the *supersonic*, *transonic*, and *hypersonic* flow regimes. Also during these years, two fundamental fluid-dynamic phenomena, namely *boundary-layer separation* and *laminar–turbulent transition*, have received significant attention from researchers.

Success in studying these and other phenomena has been facilitated by the development of modern *asymptotic methods*. These are now an inherent part of applied mathematics, but it was fluid dynamics where various asymptotic techniques, including the *method of matched asymptotic expansions*, were first formulated and used. Keeping this in mind, we start Part 2 of this series with a discussion of the mathematical aspects of the asymptotic theory. This is followed by an exposition of the results of inviscid flow theory, starting with *thin aerofoil theory* for incompressible and subsonic flows, steady and unsteady. Then we turn our attention to the properties of supersonic flows, where the linear Ackeret theory is followed by second-order Buzemann analysis. Both the flow near the aerofoil surface and in the far field are discussed. Part 2 also includes a discussion of the properties of *transonic* and *hypersonic* inviscid flows. We will conclude Part 2 with a brief discussion of viscous low-Reynolds-number flows.

Part 3 is devoted to the theory of high-Reynolds-number fluid flows. We first consider a class of flows that can be described in the framework of classical boundary-layer theory. These include the Blasius flow past a flat plate and the Falkner–Skan solutions for the flow over a wedge surface. We also discuss the Chapman shear-layer flow and Schlichting's solution for the laminar jet. Among other examples are Tollmien's solution for the viscous wake behind a rigid body and the periodic boundary layer on the

surface of a rapidly rotating cylinder. This is followed by a discussion of the properties of compressible boundary layers, including hypersonic boundary layers, which are known to involve extremely strong heating of the gas near the body surface. We then turn our attention to the phenomenon of flow separation from a rigid-body surface, which cannot be described in the framework of classical boundary-layer theory. Instead, one has to use the *viscous–inviscid interaction* concept, also known under the name of the *triple-deck model*. We first formulate the triple-deck theory in application to self-induced boundary-layer separation in supersonic flow, and then use it to describe the incompressible flow near the trailing edge of a flat plate. This is followed by an exposition of other applications, including incompressible flow separation from a smooth body surface and *marginal separation theory*, which describes flow separation at the leading edge of a thin aerofoil.

Part 4 of the series is devoted to *hydrodynamic stability theory*, which serves to predict the onset of *laminar–turbulent transition* in fluid flows. Similar to Part 3, we start with the classical results. We introduce the concept of linear instability of fluid flows, and formulate the Orr–Sommerfeld equation, which describes the stability properties of *parallel* and *quasi-parallel* flows, such as boundary layers. We also discuss the stability properties of 'inviscid flows' governed by the Rayleigh equation. This is followed by an exposition of the results of the application of the theory to various flows. Then we turn our attention to more recent developments, including *receptivity theory* and *nonlinear stability theory*. Receptivity theory is now an integral part of the theoretical predictions of laminar–turbulent transition in aerodynamic flows. It deals with the process of excitation of instability modes in the boundary layer, namely, the generation of Tollmien–Schlichting waves, cross-flow vortices, and Görtler vortices, resulting from the interaction of the boundary layer with external perturbations, for example acoustic noise, free-stream turbulence, or wall roughness. Finally, the nonlinear stability of fluid flows will be discussed, including the Landau–Stuart weakly nonlinear theory, and the derivation of the Ginzburg–Landau equation. We conclude Part 4 with a discussion of linear and nonlinear critical layers.

The present Part 1 is aimed at giving an introduction to fluid dynamics, and to prepare the reader for the more advanced material in Parts 2, 3, and 4. The book series is based on courses given by the authors over a number of years at the Moscow Institute of Physics and Technology, the University of Manchester, and Imperial College London. In fact, the majority of the material follows closely the actual lecture notes, and is supplemented with Exercises that have been used in problem classes.

Our observation is that the students find it helpful when the results of the theoretical analysis of fluid motion are compared with experiments. We make such comparisons, where appropriate, throughout the book series. Every effort has been made to contact the holders of copyright in materials reproduced in the book. Any omissions will be rectified in future printings if notice is given to the publisher.

Contents

Introduction

The history of theoretical fluid dynamics dates back over 250 years, originating in 1755, when Euler derived the differential equations describing the 'frictionless' motion of an incompressible fluid. Euler was the first to recognise the importance of the pressure forces acting inside the moving fluid, but he disregarded the forces of internal viscosity. The 'viscous' fluid dynamic equations, known as the Navier–Stokes equations, were later deduced by Navier (1827), Poisson (1831), Saint-Venant (1843), and Stokes (1845).

As with any other branch of physics, it was through a combination of experimental observations and theoretical reasoning that the principal concepts of fluid dynamics (such as the continuum description of a moving fluid) were introduced, and the equations of fluid motion were derived. One might presume that once the governing equations became known, the analysis of various fluid flows could be conducted mathematically by solving these equations. This, of course, did not happen, since a direct solution of the Navier–Stokes equations proved to be very difficult except for a limited number of cases for which *exact solutions* were possible; see Chapter 2. This difficulty is a reflection of the fact that fluid flows are rather complex and also rich in their diversity. Consequently, to achieve progress in understanding fluid flow behaviour, appropriate simplification in the mathematical formulation of the problem reflecting the physical nature of the flow being considered is required.

In order to demonstrate how this works, let us consider, as an example, the jet that forms when a fluid such as water escapes from a large container through an orifice equipped with a mouthpiece as shown in Figure I.1(a). We shall assume that the mouthpiece is symmetric and composed of two flat plates, AB and $A'B'$, with the container being on the left of A and A'. This flow was first studied by Helmholtz (1868) with the aim of comparing it with the electrostatic field between two charged plates; see Figure I.1(b). The electric field potential φ is known to satisfy the Laplace equation

$$\nabla^2 \varphi = 0 \tag{I.1}$$

everywhere outside the plates AB and $A'B'$. If the plates are good electrical conductors (such as a metal), then the potential will be constant along each plate, which means that equation (I.1) should be solved with the boundary conditions

$$\varphi = \begin{cases} 0 & \text{on } AB, \\ Q & \text{on } A'B'. \end{cases} \tag{I.2}$$

Here the potential has arbitrarily been taken equal to zero on AB, and the difference Q in the potential between AB and $A'B'$ depends on the electrical charge distribution on the plates. The solution of the boundary-value problem (I.1), (I.2) is shown in Figure I.1(b) in the form of equipotential lines.

Let us now turn our attention to the fluid flow in Figure I.1(a). It is known that in many flows the internal viscosity of the flow is very small. For example, in the jet created with a teapot spout, the viscous forces are thousands of times smaller than the pressure forces. We shall show in Chapter 3 that if the viscosity of the fluid is disregarded, then one can investigate the flow by solving the Laplace equation

$$\nabla^2 \psi = 0 \tag{I.3}$$

for the stream function ψ. The main property of the stream function is that the lines of constant ψ represent the trajectories of the fluid particles. Therefore, keeping in mind that the fluid moves along the plates AB and $A'B'$, one can write the boundary conditions for (I.3) as

$$\psi = \begin{cases} 0 & \text{on } AB, \\ Q & \text{on } A'B', \end{cases} \tag{I.4}$$

with Q now representing the rate of fluid flux through the mouthpiece.

The two mathematical problems (I.1), (I.2) and (I.3), (I.4) are absolutely equivalent. The solution of (I.1), (I.2) shown in Figure I.1(b) correctly models the physical situation for an electric field between the two plates. A 'mathematician' could expect the trajectories of the fluid particles in the jet (Figure I.1a) to coincide with the equipotential lines in Figure I.1(b). However, an 'experimentalist' and, in fact, anyone who has observed how tea is served, would disagree. The observations clearly show that the flow through a mouthpiece does not exhibit the pattern shown in Figure I.1(b). The fluid is never observed to turn around the edges of the flat plates at B and B',

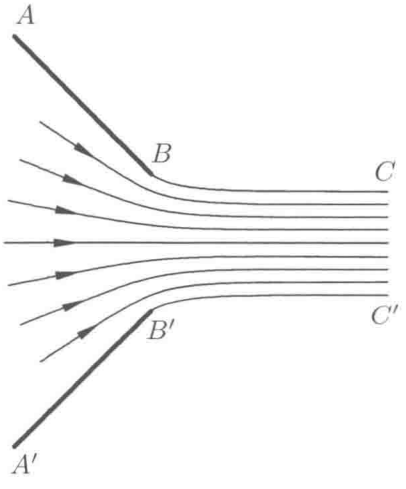

(a) Streamlines in the incompressible fluid flow through a mouthpiece composed of two flat plates AB and $A'B'$.

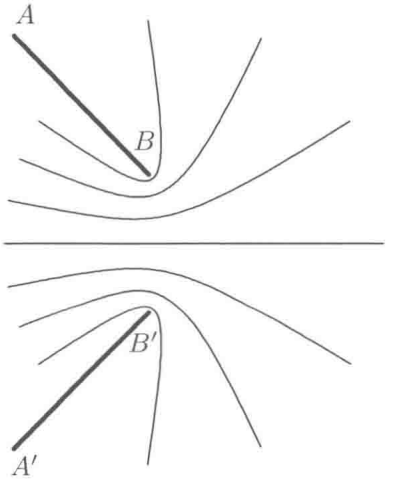

(b) Equipotential lines in the electrostatic field between two flat plates AB and $A'B'$.

Fig. I.1: Comparison of the electrostatic field between two semi-infinite flat plates with the corresponding fluid flow.

and flow back over the external surfaces AB and $A'B'$. Instead, the flow separates at points B and B' to form a confined jet surrounded by the ambient air.

This dilemma led Helmholtz to a conjecture that, in addition to the smooth solution shown in Figure I.1(b), the Laplace equation also allows for a solution where the fluid velocity has a jump across the boundaries of the jet, BC and $B'C'$ (see Figure I.1a). We shall discuss these types of solutions in Section 3.8. Helmholtz further argued that it is the fluid viscosity that, despite being very small, is responsible for global changes in the fluid motion.

In the history of fluid dynamics, there have been many episodes like these, when the alliance of theory and experiment has led to novel concepts and ideas. About fifty years ago, a new member of the alliance emerged, computational fluid dynamics (CFD). It relies on numerical solution of the Navier–Stokes equations as a means of studying the behaviour of fluid flows. At the beginning, some researchers called this approach 'numerical experimentation', and speculated that it could become a substitute for real experiments; the latter were known to be very expensive, especially when large-scale wind tunnels were involved. There were others who believed that with the development of CFD the role of theory would diminish. It is, of course, true that over the years CFD has become a powerful tool. However, both experiments and theory retain their importance. In particular, theory remains, and always will, an ideal instrument for uncovering the fundamental physical processes behind observed fluid flow behaviour. It also remains the preferred way of presenting the subject of fluid dynamics to students.

In this book series we shall mainly rely on theoretical fluid dynamics, although some elements of CFD will be introduced where this is useful for the presentation of the material.

1
Fundamentals of Fluid Dynamics

1.1 The Continuum Hypothesis

Theoretical fluid dynamics is a subdivision of continuum mechanics and as such does not attempt to describe either the molecular structure of a medium or the motion of individual molecules.[1] The continuum models matter that is sufficiently dense such that averaging over a very large number of molecules permits a meaningful definition of macroscopic quantities. Of course, this approach has certain inherent restrictions, and these may be expressed in terms of the *Knudsen number*.

Let us consider fluid flow past a rigid body, say a sphere as sketched in Figure 1.1, and try to determine the *density* of the flowing matter. The density ρ is defined as the ratio of the mass $m_{\mathcal{D}}$ to the volume $\tau_{\mathcal{D}}$ contained in a region $\mathcal{D}$ inside the flow. If there were no variation of density throughout the flow field then the region $\mathcal{D}$ could be chosen arbitrarily. However, many fluids of practical interest are compressible and undergo density changes as they move. For example, for the situation shown in

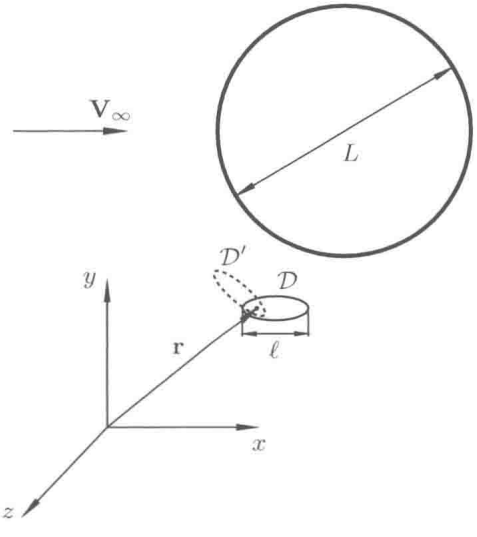

Fig. 1.1: Calculation of density $\rho(\mathbf{r}, t)$ at point $\mathbf{r}$ and time t in a fluid flow.

[1] It should be noted the Navier–Stokes equations governing fluid motion may be derived not only using the continuum mechanics approach as described in this book, but also based on the *Boltzmann equation* of the kinetic theory of gases, which treats fluid flow as the motion of an assemblage of molecules.

Figure 1.1, the fluid experiences deceleration near the front part of the sphere as it approaches from upstream, resulting in a process of compression. As the fluid subsequently moves around the sphere, it undergoes acceleration and a process of expansion. This is followed by a second compression occurring as the fluid decelerates near the rear portion of the sphere. The characteristic length scale associated with these variations coincides with the diameter L of the sphere. Therefore, in order to define the density, it is necessary to first choose an observation point in the flow. In Figure 1.1 this is denoted by the radius vector $\mathbf{r}$. This point must then be surrounded by region $\mathcal{D}$, whose characteristic length scale ℓ is small compared with L. The density at point $\mathbf{r}$ and time t is then evaluated as

$$\rho(\mathbf{r}, t) \approx \frac{m_{\mathcal{D}}}{\tau_{\mathcal{D}}}. \tag{1.1.1}$$

Formula (1.1.1) becomes progressively more accurate as the region $\mathcal{D}$ is made smaller, and a more precise definition of *density* should be written in the form

$$\rho(\mathbf{r}, t) = \lim_{\ell \to 0} \frac{m_{\mathcal{D}}}{\tau_{\mathcal{D}}}. \tag{1.1.2}$$

Thus the question of whether the concept of a continuum is useful in a particular flow becomes a question of whether the limit in equation (1.1.2) exists.

In general, the variations of $m_{\mathcal{D}}/\tau_{\mathcal{D}}$ with decreasing ℓ are quite complex, as shown schematically in Figure 1.2. When ℓ is comparable to the body scale L, then $m_{\mathcal{D}}/\tau_{\mathcal{D}}$ is found to be dependent not only on the volume $\tau_{\mathcal{D}}$, but also on the shape of region $\mathcal{D}$. If this region is stretched to the front of the cylinder (like region $\mathcal{D}'$ shown by the dashed line in Figure 1.1) then formula (1.1.1) will obviously overestimate the real density at point $\mathbf{r}$; if, on the other hand, it is stretched towards a region where the fluid experiences an expansion (solid line in Figure 1.1) then (1.1.1) will underestimate the density. This is illustrated in Figure 1.2, where the solid curve corresponds to region $\mathcal{D}$ in Figure 1.1 while the dashed line corresponds to region $\mathcal{D}'$.

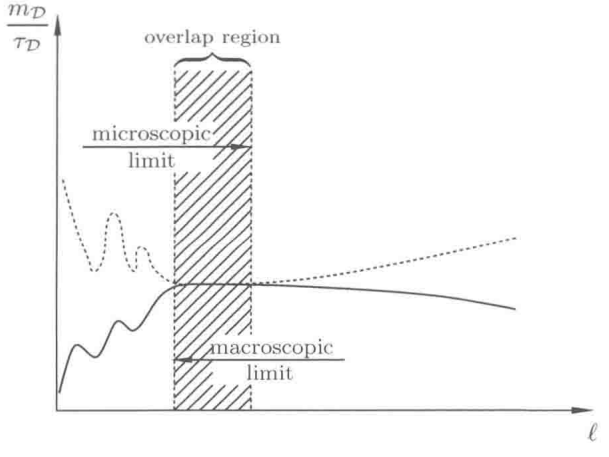

Fig. 1.2: Variations of $m_{\mathcal{D}}/\tau_{\mathcal{D}}$ for different possible shapes of region $\mathcal{D}$. Here the solid and dashed lines represent the solid and dashed shapes of region $\mathcal{D}$ in Figure 1.1.

For a fluid medium that is sufficiently dense, the apparent density as measured with various shapes of region $\mathcal{D}$ converge to the same value as $\tau_{\mathcal{D}}$ shrinks to the observation point $\mathbf{r}$, thereby indicating the existence of the limit in equation (1.1.2). However, this limit is only an intermediate *macroscopic limit* since a further decrease in region $\mathcal{D}$ eventually reveals complex fluctuations in the apparent density, which are associated with chaotic motions at the molecular level; by this stage $\tau_{\mathcal{D}}$ is so small that any measurement of $m_{\mathcal{D}}$ is strongly dependent on the number of molecules that happen to be in $\mathcal{D}$ at instant t, and therefore the fluctuations are also time-dependent. Oscillations, such as those depicted in Figure 1.2, would be recorded when ℓ becomes small enough that it is comparable to the *molecular mean free path*, λ. Here λ is defined as the average distance an individual molecule travels in a gas before colliding with another molecule. Thus the macroscopic intermediate limit (see Figure 1.2) exists only if ℓ is small with respect to L, but at the same time large with respect to λ, namely

$$\lambda \ll \ell \ll L. \tag{1.1.3}$$

The density $\rho(\mathbf{r}, t)$ may also be defined from a *microscopic point of view* as follows. If $N_{\mathcal{D}}$ denotes the number of molecules contained at time t within region $\mathcal{D}$ and m_0 is the average mass of an individual molecule then

$$\rho(\mathbf{r}, t) = \frac{m_0 N_{\mathcal{D}}}{\tau_{\mathcal{D}}}. \tag{1.1.4}$$

It is known from statistical thermodynamics that chaotic fluctuations in the apparent value of ρ that can occur as molecules pass in and out of the measuring region $\mathcal{D}$ do not influence the values of macroscopic quantities provided that the system of molecules being considered is large enough. Thus formula (1.1.4) should be more precisely written as

$$\rho(\mathbf{r}, t) = \lim_{N_{\mathcal{D}} \to \infty} \frac{m_0 N_{\mathcal{D}}}{\tau_{\mathcal{D}}}. \tag{1.1.5}$$

The process indicated in equation (1.1.5) is called the *microscopic limit* and again must be interpreted as an intermediate one. It should be noted here that the notation '$N_{\mathcal{D}} \to \infty$' does not actually imply that $N_{\mathcal{D}}$, and therefore the region $\mathcal{D}$, must become indefinitely large. To avoid performing an average for the density over a region whose size ℓ is comparable to the body scale L, the restriction $\ell \ll L$ must still be observed.

Formulae (1.1.2) and (1.1.5) give the same result in the so-called *overlap region* (see Figure 1.2) where both restrictions in (1.1.3) are observed.[2] The *Knudsen number* is defined by

$$Kn = \frac{\lambda}{L},$$

and it immediately follows from (1.1.3) that Kn must be small compared with unity. Alternatively, if $Kn \ll 1$ then any point in the flow may be surrounded by a small region whose characteristic length scale ℓ satisfies the conditions (1.1.3). Being considered as a material fragment of the moving medium, such a region represents the

[2]For a detailed discussion of the notion of overlap region, the reader is referred to Part 2 of this book series.